Analysis of the Vibration Spectrum Based on the Input Voltage Spectrum

Mathe, Laszlo; Jakobsen, Uffe; Rasmussen, Peter Omand; Pedersen, John Kim

Published in:
Proceedings of the Energy Conversion Congress and Exposition, ECCE 2009.

DOI (link to publication from Publisher):
10.1109/ECCE.2009.5316167

Publication date:
2009

Document Version
Publisher's PDF, also known as Version of record

Analysis of the Vibration Spectrum Based on the Input Voltage Spectrum

Laszlo Mathe, Uffe Jakobsen, Peter Omand Rasmussen, John K. Pedersen
Institute of Energy Technology; Aalborg University; Aalborg, Denmark
lam@iet.aau.dk

Abstract —**Pulse width modulation, present in most drives, gives rise to harmonics in the current and this generates radial forces that cause vibrations in the motor shell. This paper derives an analytical expression for the estimation of the spectrum of the radial force in a machine with an air gap, based on the spectrum of the applied voltage. The measurements show that the spectral components are caused mainly by the modulation, which agrees with the results from the analytical solution. A method to determine the dominant frequency components from the radial force spectrum based on current measurements is also presented.**

I. INTRODUCTION

Noise from an electric machine may arise due to mechanical, aerodynamic, electronic and magnetic sources [1]. The magnetic source and the mechanical structure interact due to the magnetic forces and the frequency response of the mechanical structure [2, 3]. It is well known that the normal components of the current dependent forces are significantly larger than the tangential components [2].

The standard approach for vibration analysis is to use DFT on the measured signals, rather than an analytical solution to find the spectra. The drawback of using DFT is that it is limited by its inputs: windowing will introduce sidelobes in the frequency domain, and aliasing will introduce non-existing frequency components. The magnitude of the signal will be influenced by the limits of the analogue to digital conversion, the physical setup of the measurements, and external noise. An analytical solution is not affected by the previously mentioned factors in its prediction of the spectral components.

A previous analytical approach for treating pulse width modulation (PWM) effects on AC-drives was presented in [4], however radial forces were not considered in that paper. The radial forces were considered also regarding harmonics in the magnetic air gap flux in [5], without an evaluation of the effects from PWM. However, at low speed, switching frequency is the dominant source of the acoustic noise generated by the machine [6, 7]. The effects from PWM were considered with regards to the radial force in [6], but the authors did not treat analytically the relationship between PWM and radial force. Radial force prediction and calculation for a PWM driven asynchronous motor using finite-element method (FEM) can be found in [8-10]. A very comprehensive overview of harmonic analysis of PWM is described in [11], where the focus is on the voltage spectrum and not radial force spectrum.

From vibration and acoustic noise point of view it is important to know the origin of the individual frequency components from their spectra, to avoid/minimize the excitation of the resonances of the entire drive system. Although in this paper the complex construction of a rotating machine was simplified to a coil, the simulations using finite-element method (FEM) and measurements show very good coincidence on the vibration spectra with an asynchronous motor. Based on the above-mentioned simplification, this paper introduces an analytical method for determining the frequency components of the normal force spectra caused by PWM. The method is based on the analytical description of the PWM-generated line to line voltage. A graphical presentation of the analytical solution is then compared to the measurements on a simplified setup and on an induction motor.

II. ANALYTICAL DETERMINATION OF THE FORCE SPECTRA

Based on [11], the line to line voltage spectrum of a there phase asymmetrical regularly sampled sine-triangle modulation can be expressed as:

$$V_{ll}(t)=\frac{4\sqrt{3}V_{dc}}{\pi}J_1\left(\frac{\omega_o}{\omega_c}\frac{\pi}{2}M\right)cos\left(\omega_o t+\frac{\pi}{6}\right)+$$
$$\frac{8V_{dc}}{\pi}\sum_{m=1}^{\infty}\sum_{n=-\infty}^{\infty}\left(\begin{array}{l}\frac{1}{q}J_n\left(q\frac{\pi}{2}M\right)sin\left((m+n)\frac{\pi}{2}\right)\times\\ sin\left(n\frac{\pi}{3}\right)cos\left((m\omega_c+n\omega_0)t-n\frac{\pi}{3}+\frac{\pi}{2}\right)\end{array}\right) \quad (1)$$

where: V_{dc} – DC-link voltage; M – Modulation index; ω_o – Modulated frequency; ω_c – Carrier frequency; J – Bessel function; m - Carrier frequency component; n - sideband harmonics of the carrier frequency; $q=m+n\left(\frac{\omega_0}{\omega_c}\right)$ for asymmetrical regular sampled PWM

Using equation (1) the analytical form of the spectrum of the normal force can be approximated. The normal force f in a not saturated coil is given by:

$$f=\frac{\psi^2}{2\mu_0 AN^2}=\frac{L^2}{2\mu_0 AN^2}\cdot i^2=k\cdot i^2 \quad (2)$$

where ψ – magnetic flux, μ_0 – magnetic permeability, A - cross sectional area of the magnetic path, N – number of wire turns, L – inductance, k – constant in time;

Since all the parameters in an ideal coil are constant, (noted as k in (2)) they can be ignored and thus represents a normalized spectra.

The flux can be expressed in function of the line voltage, ignoring nonlinearities and the phase resistances:

$$\psi(t) \simeq \int V_{ll}(t)dt \tag{3}$$

Expressing the flux by integrating the voltage equation (1) in function of time:

$$\psi(t) = \int V_{ll}dt = \frac{4\sqrt{3}V_{dc}}{\pi\omega_0} J_1\left(\frac{\omega_o}{\omega_c}\frac{\pi}{2}M\right)\sin\left(\omega_o t + \frac{\pi}{6}\right) + \frac{8V_{dc}}{\pi}\sum_{m=1}^{\infty}\sum_{n=-\infty}^{\infty}\left(\begin{array}{l}\frac{1}{q(m\omega_c + n\omega_o)} J_n\left(q\frac{\pi}{2}M\right)\times \\ \sin\left((m+n)\frac{\pi}{2}\right)\sin\left(n\frac{\pi}{3}\right)\times \\ \cos\left((m\omega_c + n\omega_o)t - n\frac{\pi}{3}\right)\end{array}\right) \tag{4}$$

Substituting the flux equation (4) in (2), the force equation becomes:

$$f(t) = \left(\begin{array}{l}\sqrt{\frac{1}{2\mu_0 AN^2}}\frac{4\sqrt{3}V_{dc}}{\pi\omega_0} J_1\left(\frac{\omega_o}{\omega_c}\frac{\pi}{2}M\right)\sin\left(\omega_o t + \frac{\pi}{6}\right) + \\ \sqrt{\frac{1}{2\mu_0 AN^2}}\frac{8V_{dc}}{\pi}\sum_{m=1}^{\infty}\sum_{n=-\infty}^{\infty}\left(\begin{array}{l}\frac{1}{q(m\omega_c + n\omega_o)} J_n\left(q\frac{\pi}{2}M\right)\times \\ \sin\left((m+n)\frac{\pi}{2}\right)\sin\left(n\frac{\pi}{3}\right)\times \\ \cos\left((m\omega_c + n\omega_o)t - n\frac{\pi}{3}\right)\end{array}\right)\end{array}\right)^2 \tag{5}$$

Recalling the amplitude values of the fundamental and the harmonic components from the force equation:

$$\begin{cases} Fund = \sqrt{\frac{1}{2\mu_0 AN^2}}\frac{4\sqrt{3}V_{dc}}{\pi\omega_0} J_1\left(\frac{\omega_o}{\omega_c}\frac{\pi}{2}M\right) \\ Harm_{(m,n)} = \sqrt{\frac{1}{2\mu_0 AN^2}}\frac{8V_{dc}}{\pi q(m\omega_c + n\omega_o)}\times \\ \qquad J_n\left(q\frac{\pi}{2}M\right)\sin\left((m+n)\frac{\pi}{2}\right)\sin\left(n\frac{\pi}{3}\right) \end{cases} \tag{6}$$

The force equation becomes:

$$f(t) = \left(\begin{array}{l} Fund\cdot\sin\left(\omega_o t + \frac{\pi}{6}\right) + \\ \sum_{m=1}^{\infty}\sum_{n=-\infty}^{\infty}\left(Harm_{(m,n)}\cdot\cos\left(\begin{array}{l} m\omega_c t + \\ n\left(\omega_o t - \frac{\pi}{3}\right)\end{array}\right)\right)\end{array}\right)^2 \tag{7}$$

In case of other modulation methods like space vector modulation (SVM), third-harmonic reference injection or discontinuous PWM (DPWM), equation (6) will be expanded with further harmonic components as they are described in [11].

Expanding the square and by using the trigonometric identities, (7) is transformed into:

$$f(t) = Fund^2\frac{1-\cos\left(2\left(\omega_o t + \frac{\pi}{6}\right)\right)}{2} + \sum_{m=1}^{\infty}\sum_{n=-\infty}^{\infty}\left(\begin{array}{l} Fund\cdot Harm_{(m,n)}\times \\ \sin\left(\begin{array}{l}(m\omega_c + (n+1)\omega_0)t + \\ (1-2n)\frac{\pi}{6}\end{array}\right) \\ Fund\cdot Harm_{(m,n)}\times \\ \sin\left(\begin{array}{l}((1-n)\omega_0 - m\omega_c)t + \\ (2n+1)\frac{\pi}{6}\end{array}\right)\end{array}\right) + \sum_{m=1}^{\infty}\sum_{i=1}^{m}\sum_{n=-\infty}^{\infty}\sum_{j=-\infty}^{\infty}\left(\begin{array}{l} Harm_{(m,n)}Harm_{(i,j)}\times \\ \left(\begin{array}{l}\cos\left(\begin{array}{l}((i-m)\omega_c + \\ (j-n)\omega_o\end{array}\right)t + \\ (n-j)\frac{\pi}{3}\end{array}\right) + \\ \cos\left(\begin{array}{l}((i+m)\omega_c + \\ (j+n)\omega_o\end{array}\right)t - \\ (n+j)\frac{\pi}{3}\end{array}\right)\end{array}\right) + \sum_{m=1}^{\infty}\sum_{n=-\infty}^{\infty}\sum_{j=n+1}^{\infty}\left(\begin{array}{l} Harm_{(m,n)}Harm_{(m,j)}\times \\ \left(\begin{array}{l}\cos\left((j-n)\omega_o t + (n-j)\frac{\pi}{3}\right) + \\ \cos\left(\begin{array}{l}(2m\omega_c + (n+j)\omega_o)t - \\ (n+j)\frac{\pi}{3}\end{array}\right)\end{array}\right)\end{array}\right) + \sum_{m=1}^{\infty}\sum_{n=-\infty}^{\infty}\left(\frac{\left(Harm_{(m,n)}\right)^2\times\left(\cos\left(2m\omega_c t + 2n\left(\omega_o t - \frac{\pi}{3}\right)\right)+1\right)}{2}\right) \tag{8}$$

Comparing the voltage equation (1) with the force equation (8), it can be concluded that:

1. the frequency of the fundamental force component will have double the frequency compared to the fundamental in the voltage spectrum

2. Since the force is proportional to the squared voltage, this gives rise to a convolution in the frequency domain. The second, the third, and the fourth line from equation (8) are the result of this convolution.

III. Simplified Experimental Setup for Evaluation of the Vibration Spectra

To isolate the effect of the PWM on the vibration spectra from the vibrations caused by the complex structure of the motor, a simplified setup with no moving parts was used. The behavior of the normal force in the induction motor can be approximated with a single coil shown in Fig. 1, as it was done similarly in [12], for a switched reluctance motor. To have the same shape of the current in the coil as in one phase of an induction motor, the coil was connected to the inverter together with two resistors as shown in Fig. 3. The transfer function between the current of the coil and the vibration on the frame of the coil depends on the mechanical structure of the coil. This transfer function has been determined using Random PWM (RPWM) [13]. RPWM has the property to distribute the discrete frequency components from the current spectrum creating a spectrum close to white noise. The current with a spectrum like white noise equally excites all the frequency components, giving the response of the mechanical structure to them in term of vibrations. The transfer function from phase current to shell vibrations of the asynchronous motor presented in Fig. 4 was measured in the same way. The advantage to determine the transfer function of the mechanical structure by measurements is that it gives a real picture about the entire mechanical system.

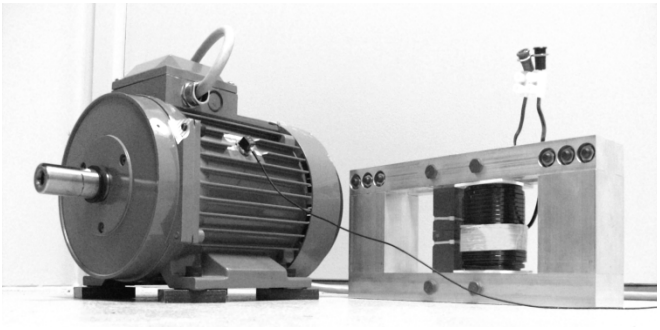

Fig. 1 The motor and coil used for measurements

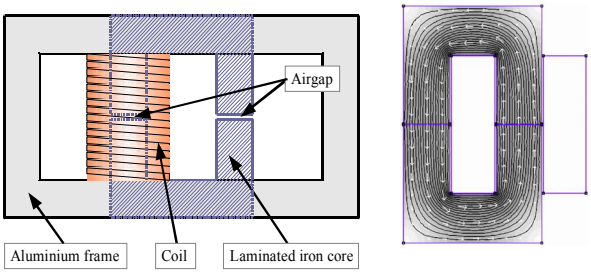

Fig. 2 On the left is shown two u-cores with an 0.8 mm air gap, and a coil to excite this core with 80 turns and 3 mH inductance. The core has a cross sectional area of 6 cm^2. The acceleration sensor is placed on the aluminum frame. The right side is a result from a FEM simulation of the magnetic circuit.

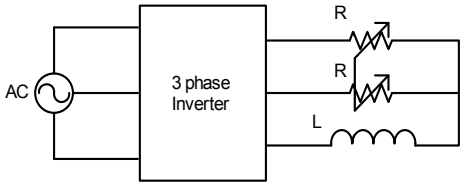

Fig. 3 Experimental setup schematic for the coil fed by an inverter

To calculate the normal force in the air gap acting on the laminated iron core of the coil, FEM simulation was set up as shown in Fig. 2. Stepping through various current levels a look up table was generated. Since vibrations comes from the acceleration on the shell of the coil, and $F = m \cdot a$ the, force is proportional to the vibrations. The normalized force spectrum is thus equal to the normalized acceleration spectrum.

IV. Experimental Validation

For experimental tests, the 2.2 kW asynchronous motor and the coil was used driven by a 2.2 kW Danfoss FC302 VLT three phase inverter. The current and vibrations on the motor/coil frame were measured with a Bruel and Kjaer Pulse Multi-analyzer type 3560. Asymmetrical regular sampled sine-triangular modulation was used for the measurements. The switching frequency was set to 5kHz, while the fundamental frequency of the current was 35Hz.

Fig. 5 presents the results of vibration spectra obtained by different methods: calculated analytically, using a current to force look-up table and by measuring the vibration on the frame of the coil. The theoretical spectra components of the vibrations created by the PWM can be seen in Fig. 5 (a) and (b). To compare the calculated and measured spectra the transfer function of the mechanical structure of the coil was added in Fig. 5 (c) and (d). The measured and calculated spectra were normalized to the maximum amplitude from their respective spectra.

To show the coincidence between the calculated and measured spectra Fig. 6 and Fig. 7 presents a zoom in the spectra around 10 kHz respectively 5 kHz.

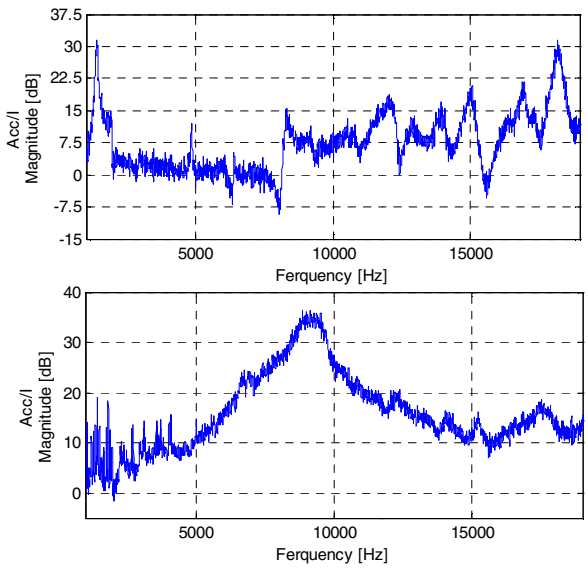

Fig. 4 Measured transfer function between current and acceleration of the mechanical structure: in the top for the coil, in the bottom for the motor

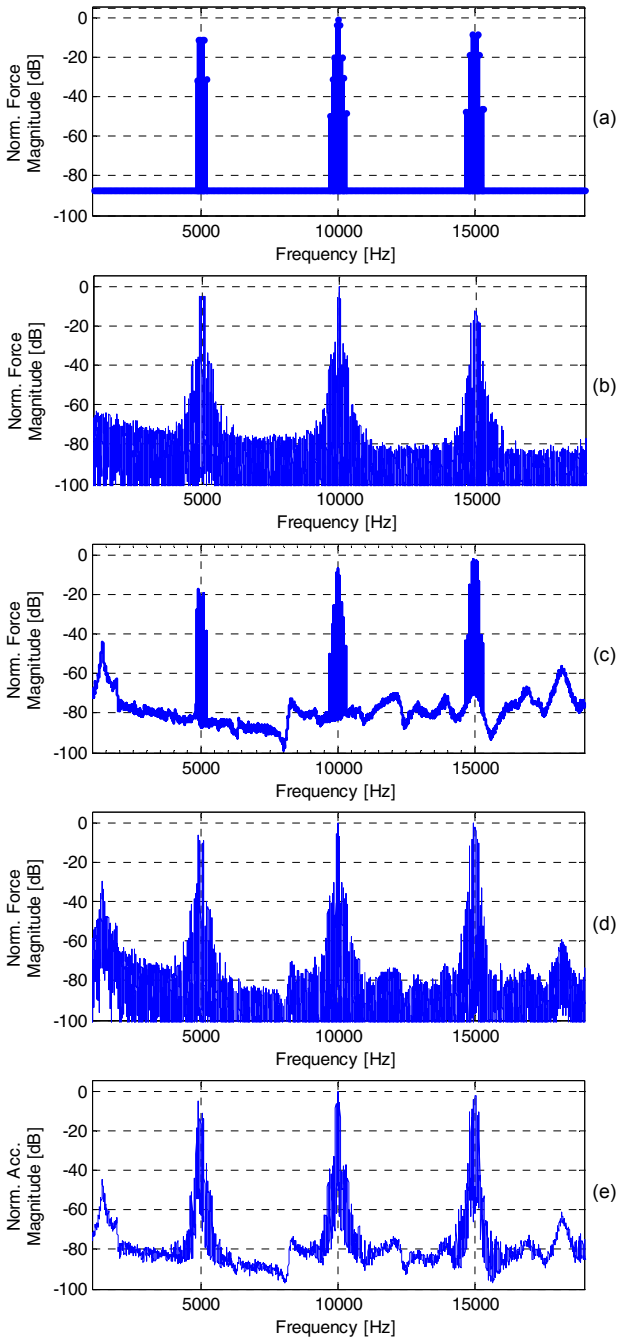

Fig. 5 The normalized vibration spectra on the frame of the coil: (a) analytical calculated spectra, (b) spectra derived using the current to force look-up table, (c) analytical calculated spectra adjusted with the transfer function of the mechanical structure, (d) Simulation using force look-up table adjusted with the transfer function of the mechanical structure (e) measured spectra

Fig. 8 presents the calculated and measured spectra for the asynchronous motor. For the spectra given by the analytical calculations (Fig. 8 (a)), the current – to – vibration transfer function of the motor has been considered. The prediction of the force spectra in the asynchronous motor using (2) is shown in Fig. 8 (b). Using (2) with the measured phase current from the rotating asynchronous motor as input, the

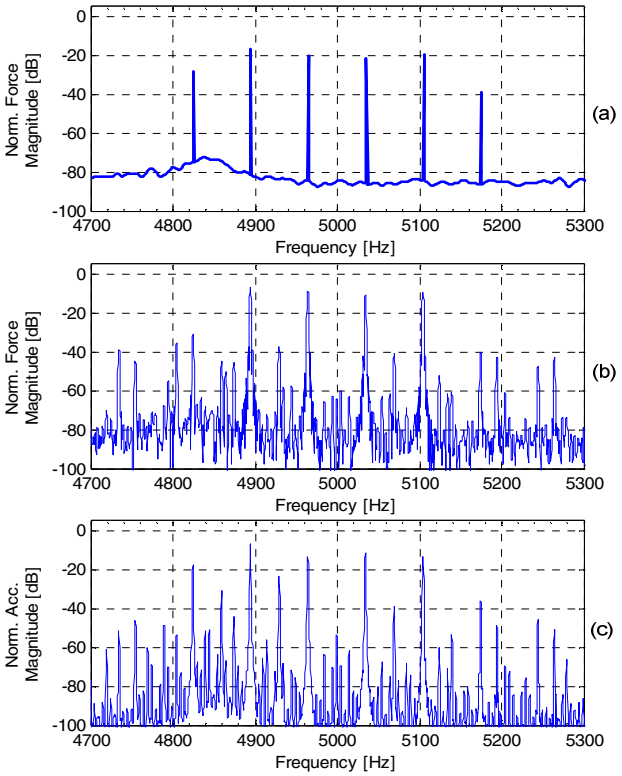

Fig. 6 Zoom in vibration spectra of the coil at 5kHz: (a) analytically calculated spectra, (b) vibration spectra using force look-up table, (c) measured vibration spectra

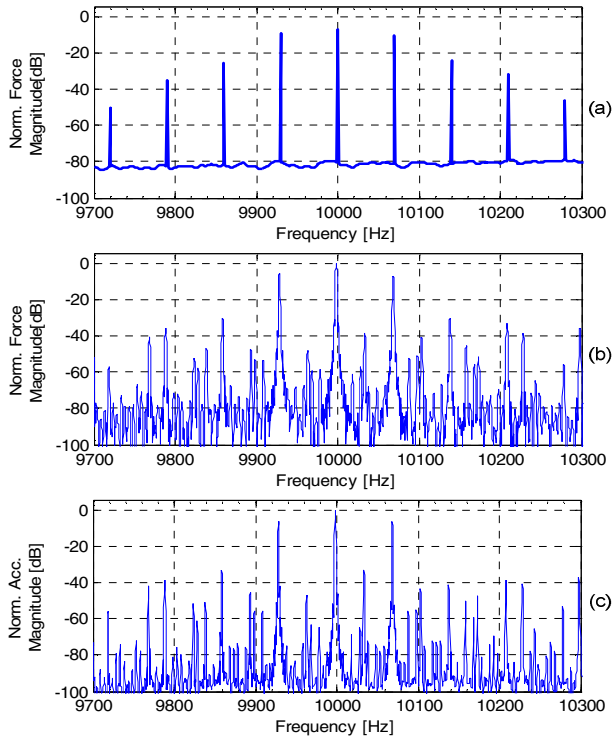

Fig. 7 Zoom in vibration spectra of the coil at 10kHz: (a) analytically calculated spectra, (b) vibration spectra using force look-up table, (c) measured vibration spectra

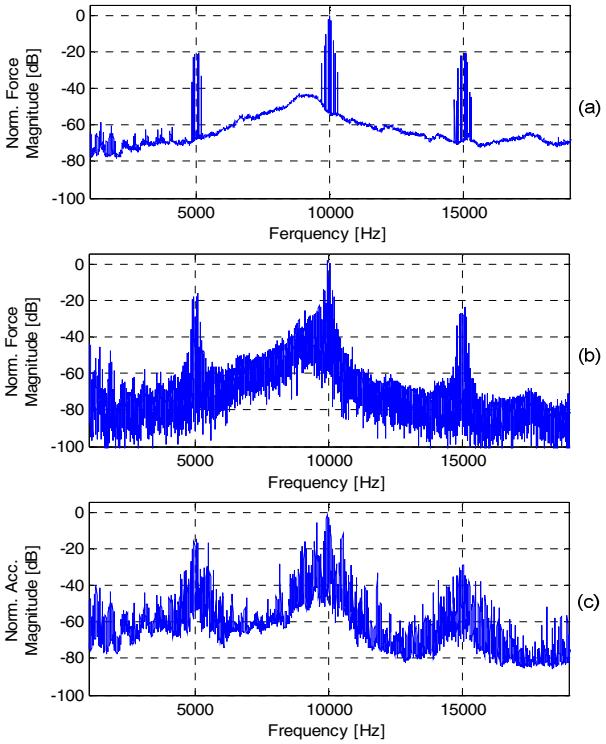

Fig. 8 The normalized spectra of vibrations on the motor shell: (a) analytically calculated spectra, (b) vibration spectra using force look-up table, (c) measured vibration spectra

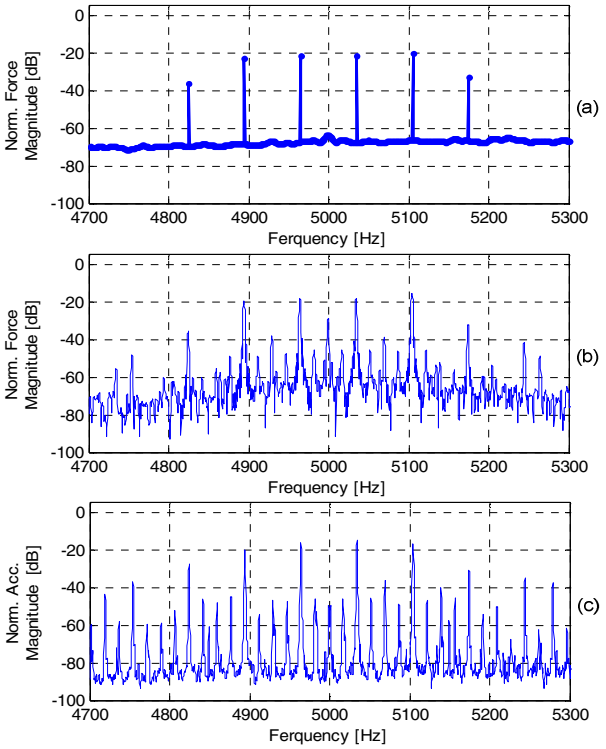

Fig. 9 Zoom in vibration spectra on the motor shell at 5kHz: (a) analytically calculated spectra, (b) vibration spectra using force look-up table, (c) measured vibration spectra

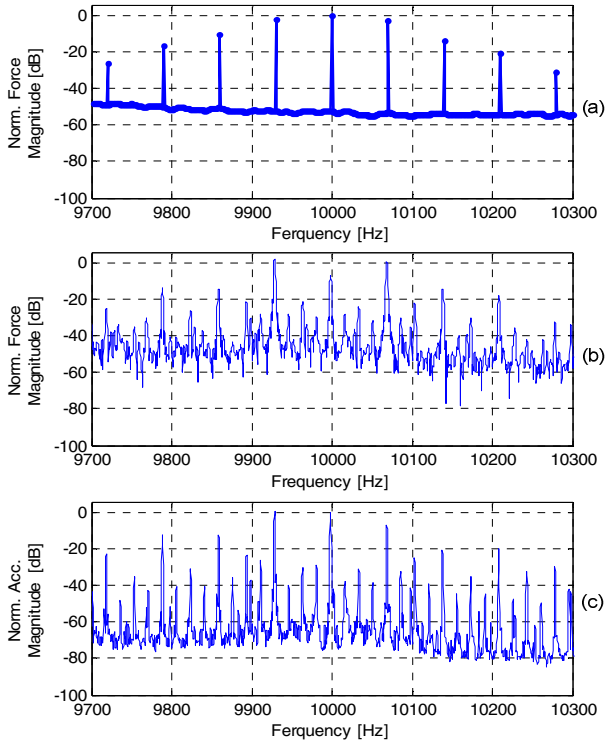

Fig. 10 Zoom in vibration spectra on the motor shell at 10 kHz: (a) analytically calculated spectra, (b) vibration spectra using force look-up table, (c) measured vibration spectra

equivalent force in the air gap of an imaginary coil was calculated and normalized. The spectrum of the force was calculated using DFT with a Hanning windowing function, the same as was used in vibration measurements on the motor shell.

As it can be seen on Fig. 8, the predicted spectra from both the analytical solution and from the FEM model, shows good agreement with the measured acceleration on the shell of the induction motor.

Although the mechanical structure of the motor is completely different from the structure of the coil used for FEM model, the spectra of the vibration around the switching frequency shows very good match.

The magnitude of vibrations on the motor and coil are influenced by mechanical parameters [12], measurement errors, and limitations of the DFT, but the main spectral components from the analytical solution fits the measured results as it is shown on the zoomed spectra. The resolution of the measurements for the zoomed spectra was increased; this is the reason why the base level of the full spectra is higher than the base level of the zoomed spectra.

V. Conclusions

New methods for predicting the spectral components of the normal force in a machine with an air gap have been presented in this paper. This prediction was achieved using a simplified setup. One solution is to analytically calculate the spectral components of the vibrations based on the analytical

solution of the line to line voltage generated by PWM. The second solution to predict the vibrations spectra is based on the measured phase current of the motor, which is fed into a current to force look-up table of the simplified system.

The measurements show that the dominant spectral components in an asynchronous motor are caused mainly by the modulation, which agrees well with the results obtained from the analytical solution and simulation based on the current to force look-up table. The advantage of the analytical method is that it allows isolating spectral components caused by the PWM even in mechanically complex drive system. The method can be applied to other than sin-triangular PWM strategies to evaluate their performance in terms of radial force. The experiments show that vibrations caused by the PWM are dominant irrespective if the PWM was applied to the coil or the induction motor.

VI. Acknowledgment

The authors would like to thank for Danfoss Drives for supporting this work.

References

[1] F. J. Gieras, C. Wang, and J. C. S. Lai, *Noise of Polyphase Electric Motors*: CRC / Taylor & Francis, 2006.

[2] R. Krishnan and P. Vijayraghavan, "State of the art: acoustic noise in switched reluctance motor drives," in *Industrial Electronics Society, 1998. IECON '98. Proceedings of the 24th Annual Conference of the IEEE*, 1998, pp. 929-934 vol.2.

[3] P. Pillay and W. Cai, "An investigation into vibration in switched reluctance motors," *Industry Applications, IEEE Transactions on,* vol. 35, pp. 589-596, 1999.

[4] H. W. van der Broeck and H. C. Skudelny, "Analytical analysis of the harmonic effects of a PWM AC drive," *Power Electronics, IEEE Transactions on,* vol. 3, pp. 216-223, 1988.

[5] S. P. Verma and A. Balan, "Determination of radial-forces in relation to noise and vibration problems of squirrel-cage induction motors," *Energy Conversion, IEEE Transaction on,* vol. 9, pp. 404-412, 1994.

[6] W. C. Lo, C. C. Chan, Z. Q. Zhu, X. Lie, D. Howe, and K. T. Chau, "Acoustic noise radiated by PWM-controllel induction machine drives," *Industrial Electronics, IEEE Transactions on,* vol. 47, pp. 880-889, 2000.

[7] N. Hashemi, R. Lisner, and D. G. Holmes, "Acoustic noise reduction for an inverter-fed three-phase induction motor," in *Industry Applications Conference, 2004. 39th IAS Annual Meeting. Conference Record of the 2004 IEEE*, 2004, pp. 2030-2035 vol.3.

[8] C. Wang, J. C. S. Lai, and A. Astfalck, "Sound power radiated from an inverter driven induction motor II: Numerical analysis," *Electric Power Applications, IEE Proceedings -,* vol. 151, pp. 341-348, 2004.

[9] C. Wang and J. C. S. Lai, "Sound power radiated from an inverter-driven induction motor. Part 3: statistical energy analysis," *Electric Power Applications, IEE Proceedings -,* vol. 152, pp. 619-626, 2005.

[10] C. Wang, A. Astfalck, and J. C. S. Lai, "Sound power radiated from an inverter-driven induction motor: experimental investigation," *Electric Power Applications, IEE Proceedings -,* vol. 149, pp. 46-52, 2002.

[11] D. G. Holmes and T. A. Lipo, *Pulse Width Modulation for Power Converters: Principles and Practice*: John Wiley &Sons, Inc., 2003.

[12] P. O. Rasmussen, J. H. Andreasen, and E. C. LaBrush, "Interlaminated damping - a method for reduction of vibration and acoustic noise for switched reluctance machines?," in *Industry Applications Conference, 2005. Fourtieth IAS Annual Meeting. Conference Record of the 2005*, 2005, pp. 1531-1539 Vol. 3.

[13] A. M. Trzynadlowski, F. Blaabjerg, J. K. Pedersen, R. L. Kirlin, and S. Legowski, "Random pulse width modulation techniques for converter-fed drive systems-a review," *Industry Applications, IEEE Transactions on,* vol. 30, pp. 1166-1175, 1994.